Identification of colon cancer intrinsic immune evasion regulons and development of reversal strategies using colon cancer organoids

Minjee Kim

Department of Medical Science

The Graduate School, Yonsei University

Identification of colon cancer intrinsic immune evasion regulons and development of reversal strategies using colon cancer organoids

Directed by Professor Hyun Seok Kim

The Master's Thesis
submitted to the Department of Medical Science,
the Graduate School of Yonsei University
in partial fulfillment of the requirements for the degree of
Master of Medical Science

Minjee Kim

December 2023

This certifies that the Master's Thesis of
Minjee Kim is approved.

Thesis Supervisor :Hyun Seok Kim

Thesis Committee Member#1 :Ho-Keun Kwon

Thesis Committee Member#2 :Byungjin Hwang

The Graduate School
Yonsei University

December 2023

<TABLE OF CONTENTS>

LIST OF FIGURES

LIST OF TABLES

ABSTRACT

Identification of colon cancer intrinsic immune evasion regulons and development of reversal strategies using colon cancer organoids

Minjee Kim

Department of Medical Science
The Graduate School, YonseiUniversity

(Directed by Professor Hyun Seok Kim)

Colorectal cancer (CRC) is a type of cancer that is known to be immune-suppressive, with only 5% of patients responding to immunotherapy. While it is important to understand how the tumor immune microenvironment (TIME) affects the effectiveness of immunotherapy, we still have limited knowledge on how cancer cells utilize certain immune-modulatory proteins to establish the surrounding immune profile. However, growing evidence suggests that the development of immunotherapy resistance in CRC occurs through distinct mechanisms depending on the intrinsic features of the cancer cells. Therefore, it is crucial to have a comprehensive understanding of the diverse immune-modulatory mechanisms that exist within the heterogeneous nature of cancer. One promising model for studying the heterogeneity of cancer is patient-derived tumor organoids, which reflect the features of the original tumor tissue.

In this study, we aim to interpret how distinct subtypes of CRC co-regulate different sets of immune-modulatory proteins, including chemokines, cytokines, and immune checkpoint ligands. By analyzing collections of CRC organoids derived from over 100 patients, along with their matched tumor tissue omics data, it is anticipated to decode the regulons of these immune-modulatory proteins and their upstream master regulators, revealinga novelapproach for more effective immunotherapy treatments.

Key words :Cancer intrinsic, Immune- modulatory regulon, Colon cancer, Organoid

Identification of colon cancer intrinsic immune evasion regulons and development of reversal strategies using colon cancer organoids

Minjee Kim

Department of Medical Science
The Graduate School, Yonsei University

(Directed by Professor Hyun Seok Kim)

I. INTRODUCTION

Colorectal cancer (CRC) is one of the most representative immune suppressive cancer subtypes, with only 5% of immunotherapy responsive group of patients[1]. Indeed, the mismatch repair proficient (pMMR) type CRC which accounts for 84% of CRC incidence is immune-excluded while the mismatch repair deficient (dMMR) type CRC, accounting for 11% of CRC incidence, harbors T cells and NK cells exhibiting high exhaustion status albeit increased infiltration of tumor-infiltrating lymphocytes (TIL).

Recent studies have identified key factors contributing to an immunosuppressive tumor microenvironment, thereby reducing the effectiveness of immunotherapies. For instance, in case of immune-exclusive pMMR type CRCs, one study found that the WNT/beta-catenin pathway's intrinsic activation in cancer cells can suppress the expression of chemokines associated with T cell recruitment[2,3]. Additionally, cancer cells can exploit cytokines and chemokines to attract immune-suppressive myeloid cells, which indirectly inhibit anti-tumorigenic T cell activity. Of another note, in immune-infiltrated tumors, the interactions between tumor-infiltrating lymphocytes (TILs) and cancer cells can give rise to immune-evasive capacity. For instance, these cancer subtypes tend to express immune-checkpoint ligands—including PD-L1, PD-L2, CEACAM-1, CD155, B7-H3, B7-H4, CD112, CD113—which can lead to T cell exhaustions[4,5,6]. They could also downregulate

MHC1 antigen presentation, hindering immune cells from recognizing and targeting malignant cells[2]. While further research is required to fully comprehend the exact mechanisms, these findings suggest that improving the effectiveness of immunotherapies for CRC patients could involve targeting the immune-modulatory pathways exploited by cancer.

CRC develop immunotherapy resistance through diverse mechanisms that depend on the intrinsic features of the cancer cells. These features include not only the distinct immune-evasive capacity, but also invasiveness, ability to metastasize, and the degree of exhibiting epithelial-to-mesenchymal (EMT)-like features. Therefore, it is essential to comprehensively understand the distinct immune modulatory mechanisms in the context of the heterogeneous nature of cancer. However, this cannot be achieved by relying on models that do not reflect the heterogeneity of cancer such as cancer cell line-based approaches. To address this challenge, a systems-level approach with the use of more complex models would be necessary to better capture the heterogeneity of cancer cells and identify key immune modulatory mechanisms that are relevant to specific subtypes of CRC.

In recent years, technical advances have addressed some limitations of simple two-dimensional cancer cell culture models by establishing a model known as three-dimensional organoid culture systems. These systems have greater similarities to the original tumor tissue in terms of their genetic features and histology[7]. In light of this, analyzing collections of cancer organoids with their matched tumor tissue would serve as an efficient means of revealing the significant factors responsible for cancer progression and immune evasion. The reason for this is the approach may provide data at the individual patient level, well-reflecting the context of cancer cell heterogeneity.

Growing evidence in the literature is suggesting a strong link between intrinsic features of cancer and the formation of the tumor immune micro-environment (TIME) surrounding it. Despite the necessity of understanding the nature of TIME to enhance the effectiveness of immunotherapies, the mechanism by which and how cancer cells exploit distinct sets of immune-modulatory proteins to alter their surrounding immune profile

remain poorly understood. It is therefore crucial to use a systemic approach with a model that could reflect the distinct characteristics of tumor tissues. This will aid in understanding the mechanisms by which an immune-suppressive TIME is established and help to overcome resistance to immunotherapy in CRC.

Therefore, in this study, I examined 103 CRC patient-derived tumor organoids that recapitulate gene expression pattern of their matched tumor to interpret the co-regulation of distinct sets of secretory proteins such as chemokines and cytokines, as well as the immune checkpoint ligands, depending on the differing intrinsic features of colorectal cancer cells. Subsequently, the co-regulation of these proteins, referred to as regulons, harboring association with distinct features of 103 colorectal cancer samples was identified. Finally, the likely upstream master-regulators that could simultaneously mitigate multiple immune modulators were suggested.

II. MATERIALS AND METHODS

1. Tumor infiltrating immune cell analysis

To estimate the abundance of distinct immune and stromal cells in 103 primary tumors, xCell was used to calculate scores for 64 types of immune and stromal cell components from tumor transcriptomics data[8]. Cell type enrichment scores were calculated with the 'xCell' package in R. Additionally, single-sample Gene Set Enrichment Analysis (ssGSEA) was utilized to calculate the enrichment score of 57 tumor microenvironment cell-associated gene signatures, which were manually collected from a literature review[9,10,11,12,13]. Additionally, to predict the immune cell activity highly relevant to immune responses against cancer, including T cell inflamed, dysfunction, exclusion status and infiltration of T cell suppressive immune cell components, Tumor Immune Dysfunction and Exclusion (TIDE) scoring method was utilized to analyze tumor transcriptomics data[14].

2. Immune subtype classification of primary tumor

103 primary tumors were classified using the Nearest Template Prediction module from Gene Pattern, following the previous report[15]. In detail, the immunogenic and non-immunogenic groups were identified based on their immune feature genes. Additionally, single-sample gene set enrichment analysis (ssGSEA) scores were calculated for manually curated immune and stromal signature gene sets. Using the 'Pheatmap' package in R, hierarchical clustering was performed with 103 samples, clustered using Euclidean distance based on the 'complete' method. The resulting tree was cut into two classes: one with high ssGSEA scores labeled as 'High immune-stromal infiltration' type and the other with low ssGSEA scores labeled as 'Low immune-stromal infiltration' type. 'Low immune-stromal infiltration' type tumors were designated as 'cold' tumors, while 'high immune-stromal infiltration' type tumors were further classified into 'exhausted' and 'active' groups, with the exhausted group being immunogenic and the active group

being non-immunogenic.

3. Immune-modulatory regulon identification

A list of immune related genes was manually selected by a thorough review of literatures and total 98 immune-modulatory genes were finally selected based on the three criteria. These included genes encoding proteins discovered with clear immune modulatory functions hence being studied as a target of immune checkpoint inhibitors such as CD274, genes with coefficient of variation value over 0.05, and finally, genes that are expressed in at least 50% of CRC patients. With these genes, spearman correlation coefficient was calculated and visualized with 'pheatmap' package in R. After confirming the immunomodulatory functions and correlation with distinct types of immune cell components, 6 different immune modulatory regulons were identified.

4. Identification of candidate master regulators of immune-modulatory regulons

Lists of transcription factor (TF) and target gene (TG) pairs has been collected from Omnipath and Human Trrust databased (TRRUST v2). Transcription factors that have at least one of the immune modulatory genes as their downstream target were selected. Then. hypergeometric test was conducted to determine the extent of overlap between genes identified within the regulon obtained through Spearman correlation analysis and the group of downstream TGs of each TF.

5. Statistical analysis

All graphs were drawn and statistical significances were tested using the R software (ver. 4.0.3).

III. RESULTS

1. Clinical features of 103 patients with colorectal cancer and the overall flow of the research

To identify and deconstruct the cancer intrinsic regulatory mechanisms of immune-related gene expression, contributing to the establishment of heterogeneous immune profiles, I conducted a comprehensive analysis using data from 103 cancer patients. Each patient was characterized by unique clinical features, including tumor location, microsatellite instability (MSI) status, stages, and recurrence (Figure 1a). Notably, the samples covered patients across various stages of CRC, ensuring a comprehensive representation from early to advanced phases of CRC tumorigenesis. Furthermore, consistent with previous findings in the colorectal cancer population, I observed a prevalence of patients with microsatellite-stable (MSS) type colorectal cancer compared to those with microsatellite instability (MSI) (Figure 1a). This suggests that the patient cohort used in our study likely reflects the common characteristics of colorectal cancer without bias.

To investigate cancer-intrinsic immune evasion mechanisms across distinct subtypes of CRC, I opted to dissect the unique immune status of CRC patients and the underlying cancer-intrinsic features contributing to it. This multifaceted analysis involved two fundamental steps: a comprehensive examination of transcriptomic data extracted from colorectal cancer patient tissues and their corresponding organoids (Figure 1b), and the identification of co-regulated set of immune regulatory genes—referred to as regulons—within cancer, along with their candidate master regulators (Figure 1c).

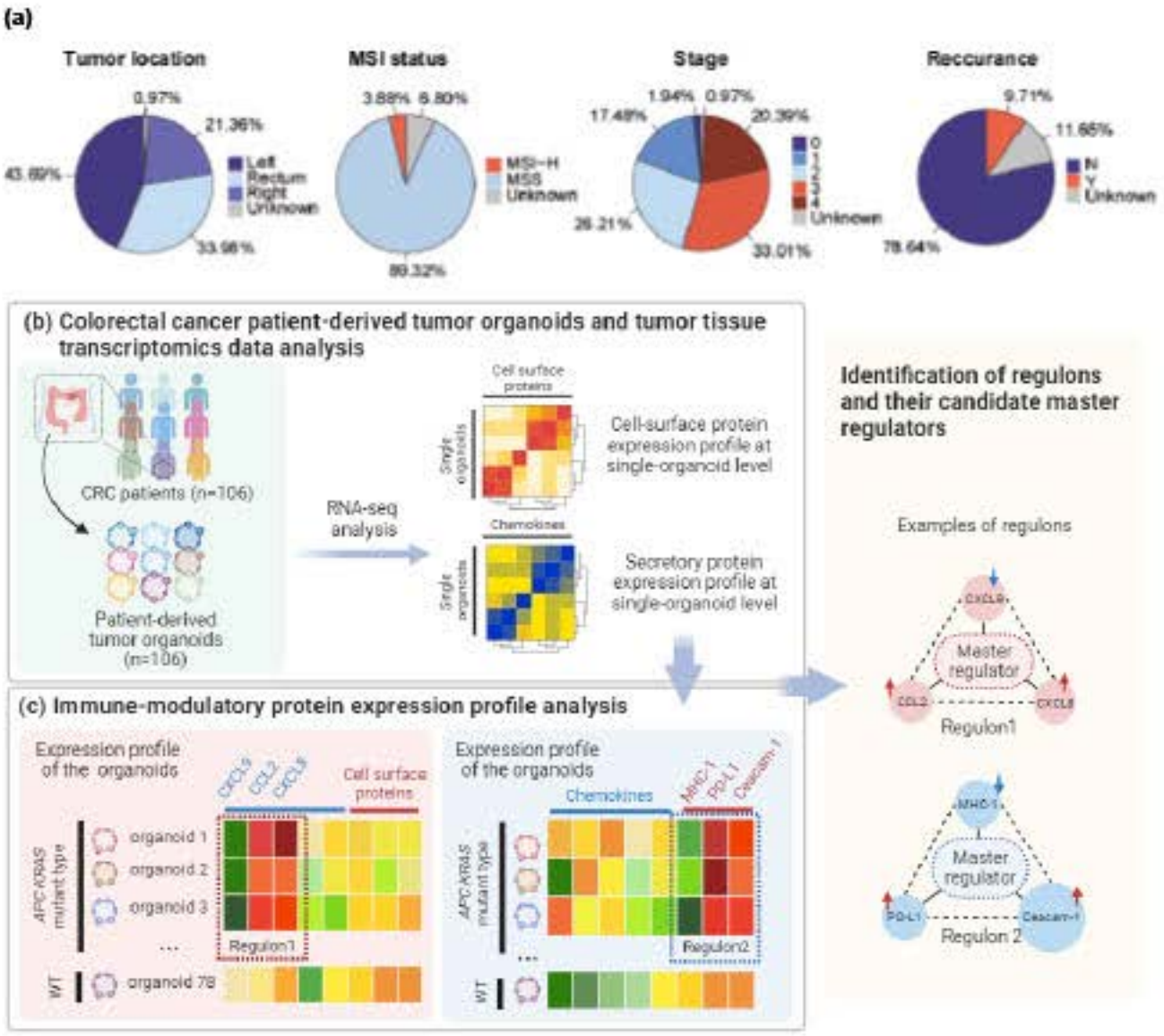

Figure 1. Characteristics of 103 Colorectal cancer (CRC) and the overall flow of the research. (a) Diagrams showing the clinical features of 103 CRC patients. (b, c) Schematic representation of the research flow.

2. The gene expression patterns of organoids match their respective tumor tissues

For further analyses, I first examined the concordance of gene expression patterns between organoids and tissues. I initially selected the top 5000 genes with the highest standard deviation in organoids. Subsequently, the Spearman correlation coefficient values between their expression levels in organoids and their corresponding tumor tissues were calculated. The results revealed a significant correlation in the expression patterns of the majority of these gene (Figure 2a). In addition to exploring genes with high variability in organoids, my focus extended to genes associated with major carcinogenesis signaling pathways, referred here to as hallmark genes. These genes were collected from the carcinogenesis-related gene sets within the hallmark gene sets v6, including DNA repair, KRAS signaling, MYC targets, PI3K/AKT/mTOR, WNT/β-catenin, NOTCH signaling, and the P53 pathway (n=1092). Again, I found a significant correlation in the expression of hallmark genes (Figure 2b). Notably, only 278 genes overlapped between the top 5000 highly variable genes and the curated hallmark genes (Figure 2c). Interestingly, a higher correlation between organoids and their matched tissues was observed with genes involved in major carcinogenesis pathways compared to the top variable genes, suggesting the conservation of oncogenic gene expression patterns of tumor tissue in the organoids (Figure 2d).

Moreover, I explored the conservation of carcinogenesis-related pathways within the organoids. Employing the hallmark gene set v6 from MSigDB, ssGSEA analysis was conducted, scoring both organoids and tumor tissues for each gene set. The Spearman correlation analysis between organoids and tissues revealed significant and positive correlations within cancer signaling pathways, such as P53, MYC, WNT/beta-catenin, epithelial-to-mesenchymal transition, DNA repair, and PI3K/AKT/MTOR signaling pathways (Figure 3). These findings collectively suggest that the intrinsic gene expression features of cancer cells in organoids effectively recapitulate those of corresponding tumors in the primary tissues.

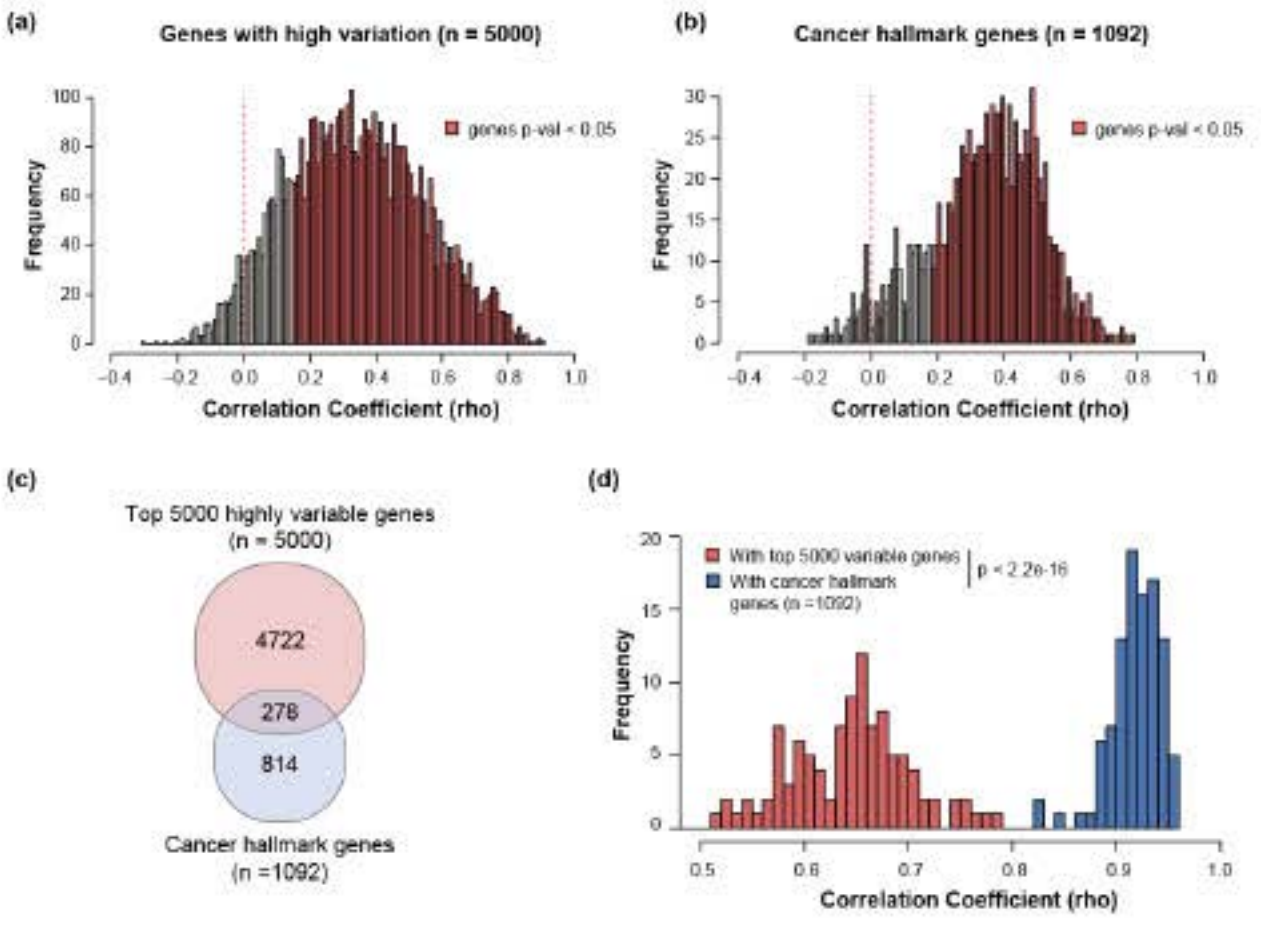

Figure 2. The gene expression pattern of organoids matches with the corresponding tumor tissue. Histogram showing correlation in the expression of individual genes included in the top 5000 variable gene set (a) and genes collected from cancer hallmark gene set (b). The Spearman correlation value was assessed between the organoids and tumor tissues, representing the relationship between the expression of a specific gene in organoids and their corresponding gene in tumor tissues. (c) Diagram showing the overlap between the top 5000 variable genes and cancer hallmark genes. (d) Histogram showing the gene expression values of all the genes within each gene set in a certain cancer patient-derived organoid to the gene expression values of the same set of genes in the matched tumor tissue, reflecting the relationship between the overall expression patterns of gene sets in each organoid compared to its matched tumor tissue across the entire dataset of 103 samples. (Wilcoxon rank-sum test was used to calculate the significance).

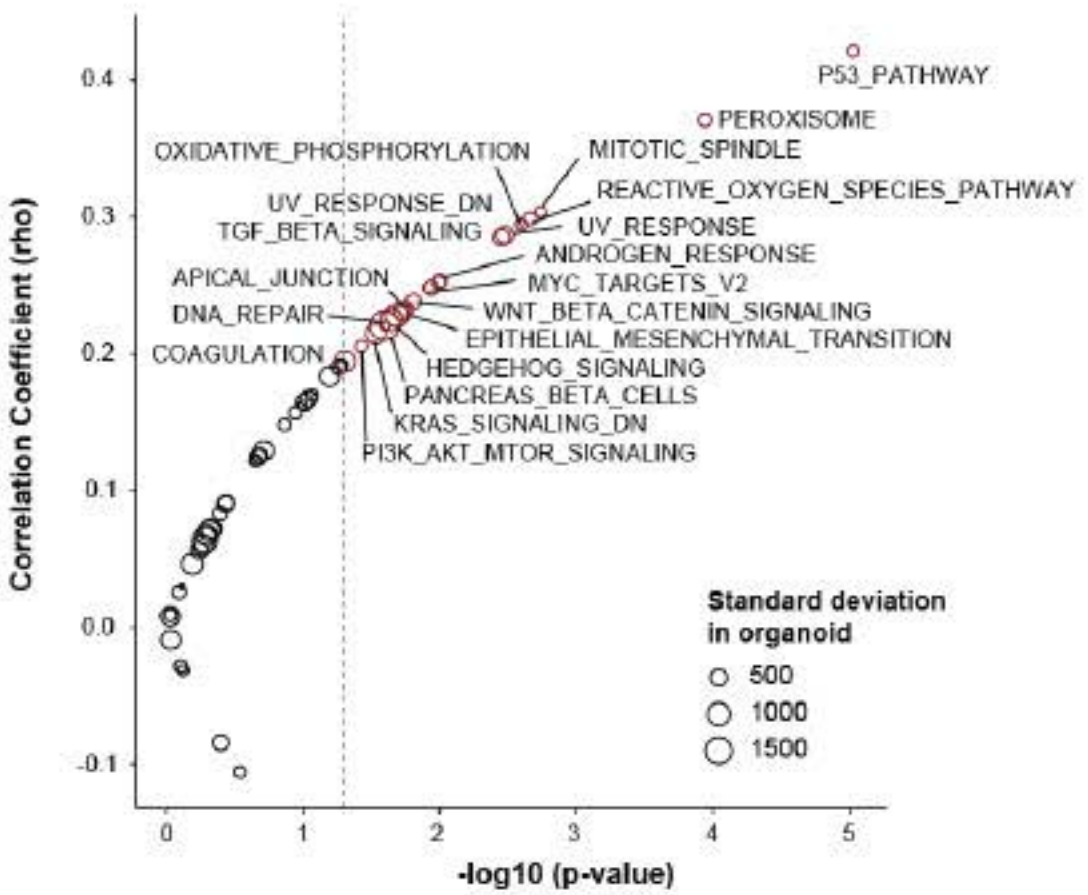

Figure 3. Carcinogenesis-related pathways observed in tumor tissues are preserved in organoids. Plot showing correlations in the major signaling pathways based on Single Sample Gene Set Enrichment Analysis (ssGSEA) calculations performed on the tumor organoids and their corresponding primary tumor tissues.

3. Immune subtype classification of 103 colorectal cancer (CRC) patients

After confirming that the organoids accurately replicated the oncogenic characteristics of tumor tissue, I proceeded to analyze the tumor immune microenvironment (TIME) profiles of 103 tumor tissues. Initially, patients were categorized into immunogenic and non-immunogenic groups based on their immune signature gene expression patterns (see Figure 4a). As anticipated, the immunogenic groups displayed a higher proportion of immune cell components compared to the non-immunogenic groups, as evidenced by the elevated 'immuneScore' calculated through xCell analysis (refer to Figure 4b). Remarkably, tumors classified as immunogenic exhibited notable enrichment in stromal cell subsets, as well as both innate and adaptive immune cell types (Figure 4b), indicating the overall active interplay among non-epithelial cell components.

To further characterize the TIME status of each tumor based on an approach that could reflect distinct TIME cell compartments, gene expression signatures associated with major TIME cell components were collected for ssGSEA score calculation. 30 TIME signature gene sets with the highest standard deviation scores were selected, encompassing both immune and stromal cell populations. This ensured the comprehensive evaluation of TIME components, involving multiple players crucial for unique TIME formation. Subsequently, hierarchical clustering analysis revealed two distinct groups: one with overall high immune-stromal cell scores, and the other group with relatively lower scores (Figure 5a). Given the immune-suppressive roles of stromal compartments, the group highly enriched with both immune and stromal cells was labeled as the ‘exhausted’ group. The remaining patients, with a relatively lower degree of non-epithelial cell infiltration, were further classified into two distinct subgroups: those with an immunogenic tumor designated as the 'active' group and those exhibiting a non-immunogenic feature labeled as the 'desert' group (Figure 5b). Intriguingly, the 'immune desert' group was mainly composed of advanced-stage cancer, while the 'active' group predominantly included early-stage tumors, demonstrating that the classification system could effectively reflect clinical

features of CRC (Figure 5c).

Considering the complexity of cellular compositions in the Tumor Immune Microenvironment (TIME) and their dynamic interactions leading to distinct immune responses against tumors[16], I examined the key features relevant to the anti-cancer immune responses in each immune subtype. These features included levels of CD8+ T cell infiltration, activation, dysfunction, as well as the infiltration of T-cell suppressive myeloid-derived suppressor cells (MDSC) and cancer-associated fibroblasts (CAF) in each patient group (Figure 6a). Consistent with data observed in ssGSEA analysis for TIME cell components (Figure 5a), the findings revealed that the immune exhausted group exhibited the highest CAF score and CD8+ T cell infiltration, indicated by high CD8+ T cell and T cell inflamed scores (Figure 6a). Intriguingly, this group also showed the highest T cell dysfunction score and CD274 score, suggesting that infiltrating T cells had been activated and tended toward a dysfunctional state (Figure 6a). In contrast, the immune desert group exhibited the lowest CD8+ T cell and T cell inflamed scores, implying a lack of T cell infiltration, which may underlie the lowest scores for indicators of T cell dysfunction status (Figure 6a). Notably, this group had the highest MDSC score, demonstrating an enrichment of immune-suppressive cell components in its TIME (Figure 6a). Additionally, the patient group with tumors exhibiting a median level of non-epithelial cell infiltration (active group) was observed to have lower T cell dysfunction and inflamed score as well as lower CAF score, despite similar level of CD8+ T cell score compared to the exhausted group (Figure 6a). These results suggest that CAF enrichment likely contributes to impairing functions of cytotoxic lymphocytes, consistent with previous reports[17].

Aligned with the fact that the immune active group showed high T cell infiltration, CAF components, and T cell dysfunction status, CMS4 cancers known for their immune-suppressive TIME enriched with both immune and stromal components were prevalent among these groups (Figure 6b). Conversely, patients with CMS2 cancers, the least immune-infiltrated among the four CMS types, were predominant in the desert group (Figure 6b). Cancer patients with an active immune status lacked CMS4-type tumors,

supporting the observations of lower immune dysfunction scores compared to exhausted groups (Figure 6b). Collectively, stratifying CRC patients into three distinct immune statuses based on signature genes representing inflammatory stromal response and patterns of infiltrated TIME components effectively captured the diverse immune landscapes of tumors, aligning with the established CRC classification system (Figure 6c).

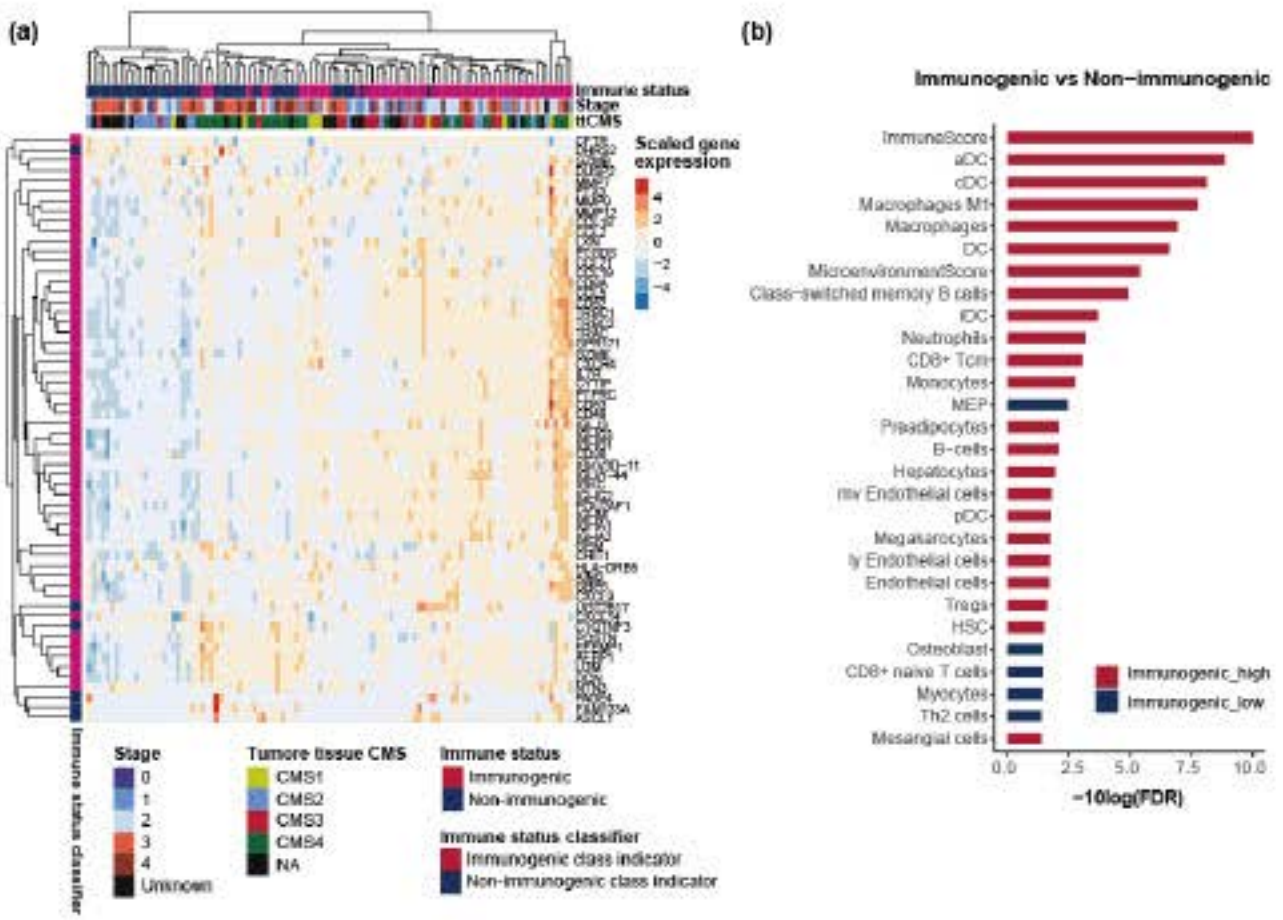

Figure 4. Immune-stromal gene signature-based tumor classification. (a) Heatmap showing the expression patterns of immune-stromal response-associated genes in the 103 primary tumor tissues. (b) Bar plot showing significantly enriched or depleted immune cell components in the immunogenic group compared to the non-immunogenic group. Patients were distinguished by the Nearest Template Prediction module based on immune-stromal response-associated genes and immune cell components were scored by analyzing bulk tumor transcriptomics data with xCell (See methods for detail).

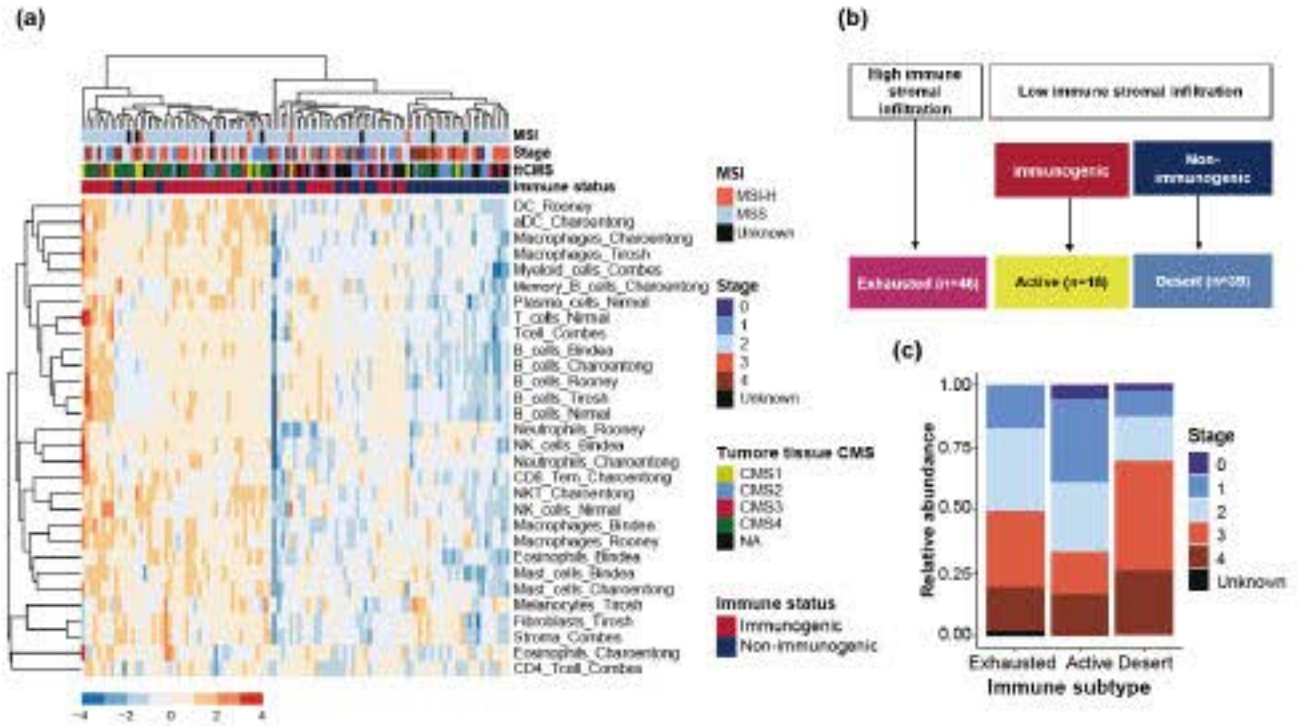

Figure 5. The immune subtype classification of CRC based on immune response gene expression and cell composition, reflects tumor clinical stage. (a) Heatmap of ssGSEA scores for 30 tumor immune-microenvironment (TIME) composing cell signature gene sets calculated from bulk transcriptomics data of 103 patients. The scores were row-wise scaled for presentation. (b) Schematic illustrating the classification of 103 colorectal cancer patients based on TIME features and predicted immunogenicity. The 'High ssGSEA score' group represents a patient cluster with an overall high score for 30 TIME-composing cell gene sets, while the 'Low ssGSEA score' group comprises the remaining patients with relatively low levels of ssGSEA scores for TIME signature gene sets. (c) Plot showing a distribution of patients with distinct tumor stages across three immune subtypes.

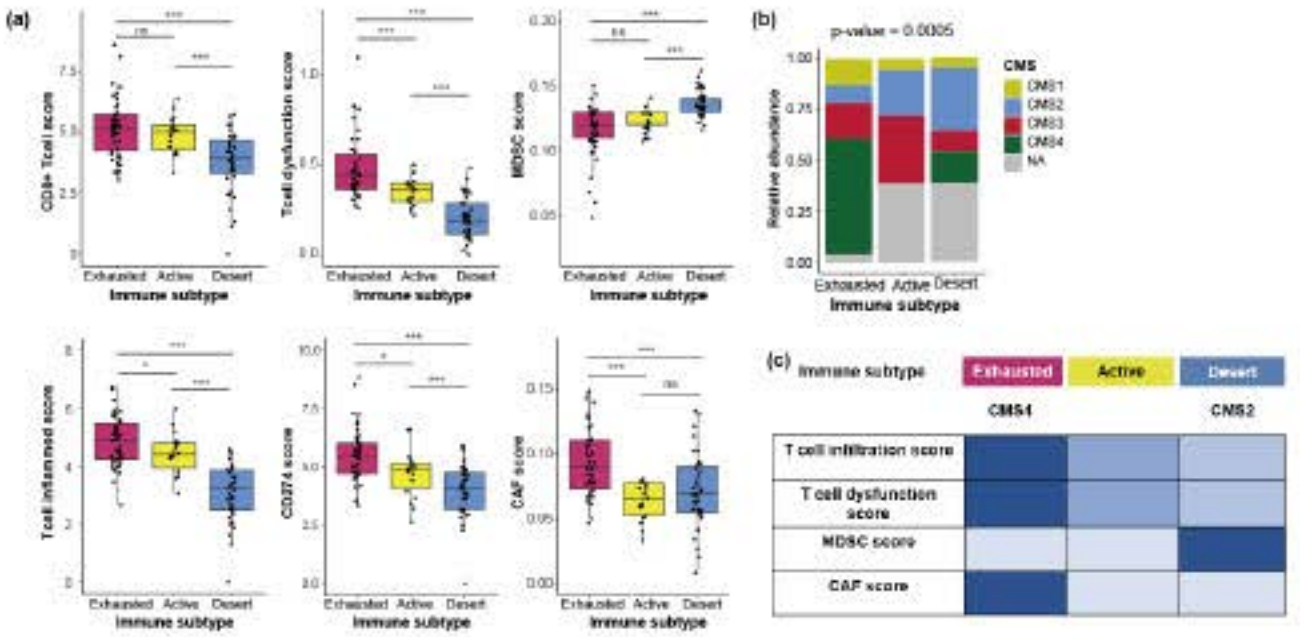

Figure 6. Distinct TIME features of CRC across the three immune subtypes. (a) Graphs depicting Tumor Immune Dysfunction and Exclusion (TIDE) scores calculated from bulk transcriptomics data of 103 patients. Differences between each group were assessed using Wilcoxon rank-sum test (ns: not significant, *p < 0.05, ***p < 0.001). The data represents mean ± SD. (b) Plots showing the distribution of CMS types within each TIME group. (One-way ANNOVA) (c) Schematic showing features of three distinct TIME classes. The darkest color denotes the highest score.

4. The three different immune subtypes of CRC exhibit distinct tumor-intrinsic features

After characterizing 103 CRC patients into three distinct classes based on their TIME states, I investigated their differences in cancer-intrinsic molecular features. I first opted to examine variations in tumor-intrinsic signaling pathway activation across the three immune subtypes. Activation levels of pathways related to hallmark gene sets and KEGG pathways were assessed through single-sample gene set enrichment analysis (ssGSEA) using transcriptomics data from patient-derived organoids (PDOs). Subsequently, pathways that exhibited differential activation in at least one of the immune subtypes were selected, employing the One-way ANOVA test to discern their activation patterns across these subtypes (Figure 7a). PDOs derived from the immune active group tended to be enriched in genes related to the p53 pathway (HALLMARK_P53_PATHWAY) while showing low activation in spermatogenesis (HALLMARK_SPERMATOGENESIS) and SNARE-mediated vesicular transport (KEGG_SNARE INTERACTIONS IN VESICULAR TRANSPORT) pathways (Figure 7a). In the case of exhausted group PDOs, they exhibited activated hedgehog signaling pathways compared to other immune subtypes (Figure 7a). Intriguingly, KEGG pathway enrichment analysis revealed PDOs of immune desert type tumors exhibit active glycerolipid metabolism pathways (Figure 7a). Taken together, these observations indicate that the distinct immune subtypes of tumors harbor a differential cancer-intrinsic signaling pathway activation pattern.

To further examine whether the signaling pathways showing distinct activation patterns within the cancer cells of different immune subtype tumors correlate with the immune response, I investigated the correlation between TIDE scores obtained from the primary tumor and enrichment scores of these pathways calculated in PDOs (Figure 7b). Notably, cancer-intrinsic P53 pathway activation exhibited a positive correlation with the T cell infiltration level of the tumor, as denoted by a significant and positive correlation with both T cell inflamed score and T cell dysfunction score (Figure 7b). Additionally,

cancer-intrinsic p53 pathway activation showed a positive correlation with the MSI signature of the tumor, suggesting an association with cancer antigenicity and the corresponding T cell antigen recognition response (Figure 7b). In contrast, the spermatogenesis pathway in cancer cells showed a clear negative correlation with the predicted MSI signature in tumor tissue, possibly explaining the lower enrichment scores in PDOs of the immune active group (Figure 7b). Of particular note, the cancer-intrinsic hedgehog signaling pathway, which had been activated in exhausted group tumor tissues, positively and significantly correlated with CD8+ T cell infiltration, CD274 level, and more critically, CAF level (Figure 7b). In consistent with previous observations that suggested the contribution of CAF to impairing cytotoxic lymphocytes (Figure 6a), these results again demonstrate the association between high CAF and T dysfunction levels in exhausted TIME. In the case of the glycerolipid metabolism pathway within CRC cells, associated with immune desert type tumors (Figure 7a), it exhibited a negative correlation with overall T cell activity, denoted by negative correlations with IFNG, T cell inflamed, and CD274 scores, while positively correlating with MDSC infiltration (Figure 7b). Overall, these findings effectively supported my hypothesis that the cancer-intrinsic features may have association with the development of unique TIME and correspondingly, the immune responses in CRC.

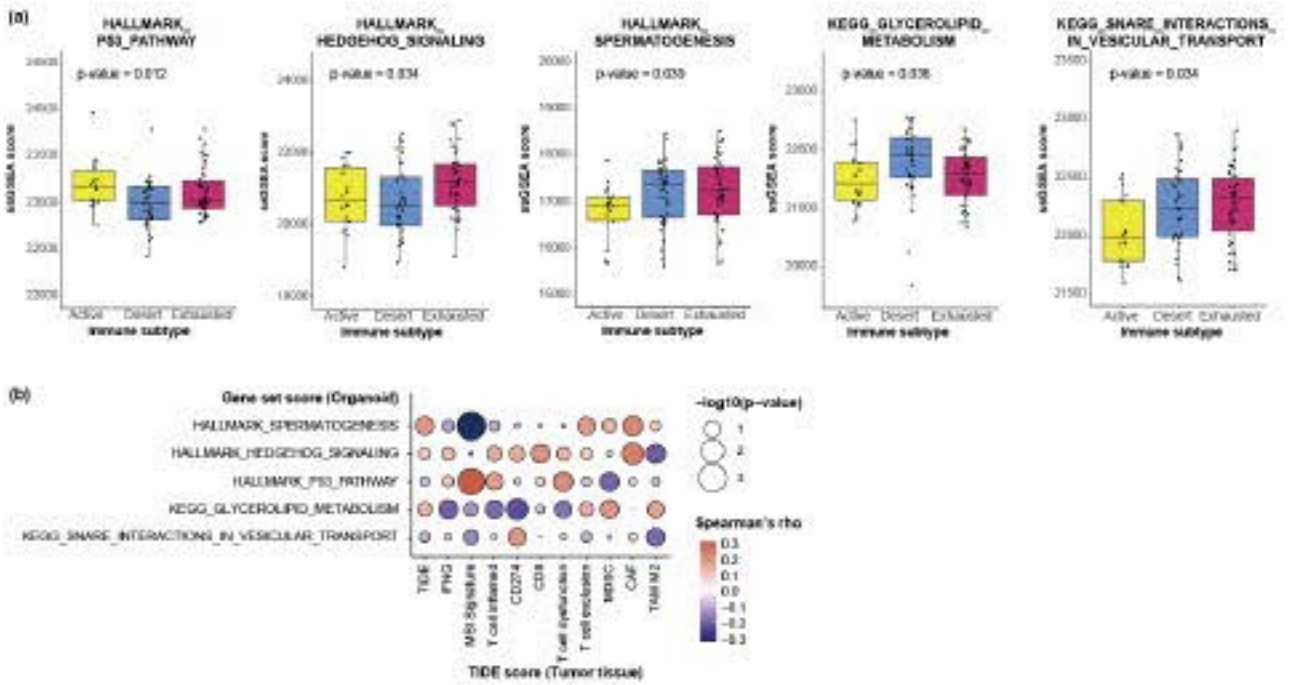

Figure 7. Distinct cancer-intrinsic features across the three immune subtypes. (a) Graphs depicting enrichment scores calculated from ssGSEA analysis with transcriptomics data of 103 patient-derived organoids. A one-way ANOVA test was conducted for significance, and the data represent mean ± SD. (b) Bubble plot showing the correlation between gene set enrichment scores calculated from the transcriptomics data of 103 patient-derived organoids and TIDE scores computed with the transcriptomics data of corresponding tumor tissues.

5. Identification of cancer-intrinsic immune-modulatory regulons

Based on the observed correlation between variable tumor-intrinsic transcriptomic features and the unique tumor immune microenvironment (TIME) along with immune responses, I investigated whether colorectal cancer (CRC) cells manifest distinct patterns of cancer cell-intrinsic immune-modulatory genes. Initially, I curated genes associated with TIME establishment and the modulation of immune cell activities, encompassing MHC class I (MHC1) and class II (MHC2) alleles, immune checkpoint receptor ligands, Interferon-stimulated genes (ISGs), chemokines, cytokines, and oncology-related protein-coding genes. To ensure relevance, I excluded genes with minimal variation or those expressed in less than 50% of cancer organoids (see methods), resulting in a refined set of 98 genes of interest (Table 1).

The global expression pattern of selected immune regulatory genes was then examined in the organoid and their matched tumor tissue, revealing extreme heterogeneity across patients (Figure 8a and 8b). Notably, despite the typical restriction of MHC2 molecule expression to specific antigen-presenting cells, certain subgroups of cancer cells exhibited relatively higher levels of MHC2 molecules compared to others (Figure 6a). Additionally, most of the genes encoding MHC1 alleles or MHC2 alleles clustered together, as expected, aligning with the well-established notion of their tightly associated regulation[18] (Figure 8a and 8b). In addition to MHC alleles, CXCL9, CXCL10, and CXCL11, chemokines identified with their roles in recruiting anti-tumorigenic T cells[19,20,21], also clustered together (Figure 8a and 8b). These observations suggested that specific immune modulatory genes could be subject to simultaneous regulation within cancer cells, which may contribute in shaping distinct tumor microenvironments (TMEs).

To explore the co-regulatory relationships among these genes, I calculated the Spearman correlation coefficient between the selected genes in the organoids, revealing an overall positive correlation relationship (Figure 9). Again, genes responsible for encoding MHC1 molecules, MHC2 molecules, and chemokines with anti-tumor properties exhibited

robust correlations with other genes in the same category, likely indicating a shared regulatory mechanism. Of particular note, the clear correlation was observed between CD74 and the genes encoding MHC2 molecules (Figure 8), aligning with the previous report that confirmed a significant correlation in the expression of CD74 and MHC2-pathway genes in the tumor tissue of triple-negative breast cancer[20]. Given the known functions of each gene and the significance of their co-regulatory relationships, 6 immune-modulatory gene expression sets were defined, namely NK-cell related regulons, MHC2 related regulons, LGALS9-related regulon, MHC1 related regulon, suppressive chemokine related regulon, and VTCN1-related regulon (Figure 9 and Table 2).

To investigate the expression pattern of the regulons, enrichment scores were calculated in both organoids and tissue samples with ssGSEA analysis. Interestingly, the regulon scores in organoids and their corresponding tissues showed no significant correlation, except for the MHC1- and MHC2- related regulon (Figure 10a). This observation led to two hypotheses. First, the expression of immune modulatory genes in cancer cells may necessitate interactions with other cell components within the TME. Second, immune modulatory genes are primarily expressed by non-cancerous cells within the TME. Indeed, a higher correlation coefficient was observed for genes included in all six regulons in the immune desert group (Figure 10b), highlighting the significant role of tumor-infiltrating cell components in shaping the overall immune-related gene expression patterns of tumor tissue.

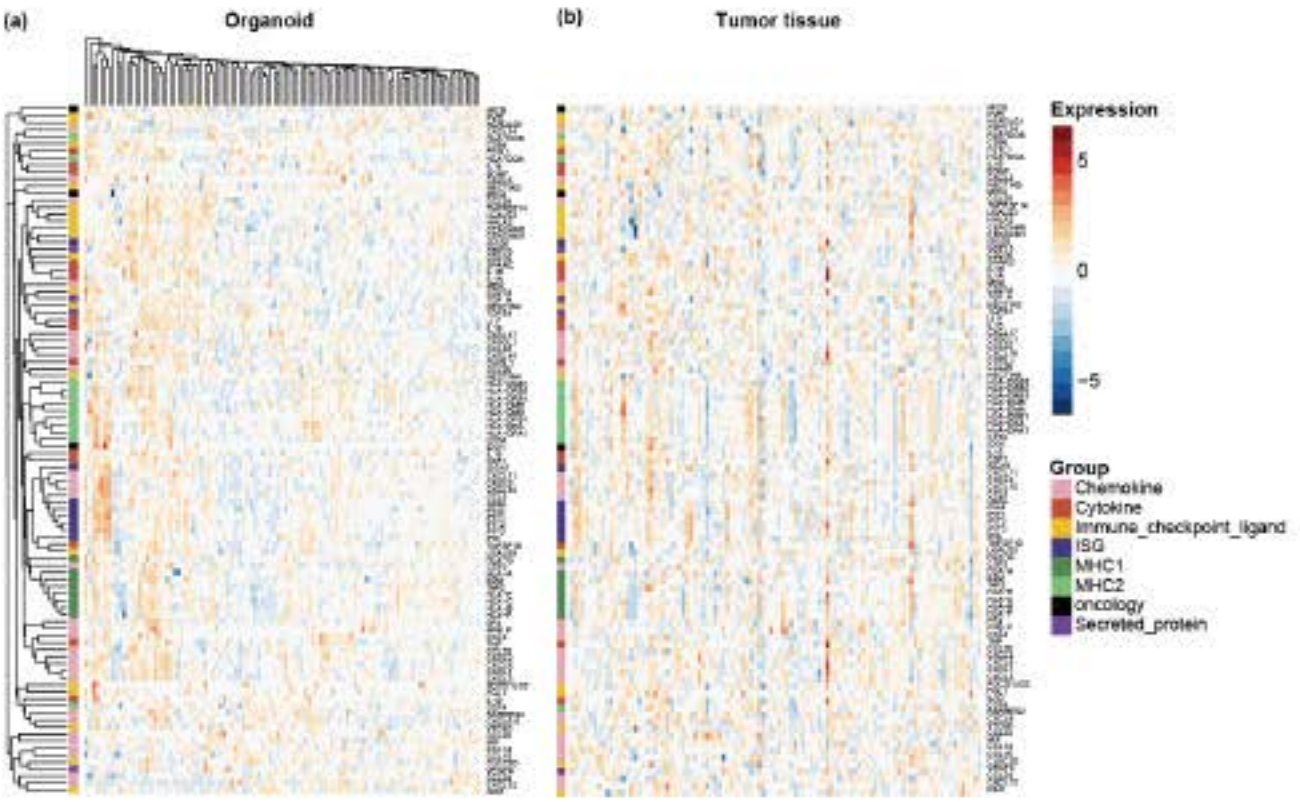

Figure 8. The expression patterns of immune modulatory genes in 103 organoids and corresponding tissues. Heatmap illustrating the heterogeneous immune-modulatory gene expression patterns in 103 (a) organoids and (b) tissues. The data has been row-wise centered, and hierarchical clustering was performed using complete linkage. Genes were clustered based on the Spearman correlation, while samples were clustered using the Euclidean distance metric. The order of patients and genes in the tissue heatmap directly corresponds to the their order established in the organoid heatmap, allowing for direct comparison of gene expression patterns between organoids and tissues.

(a)

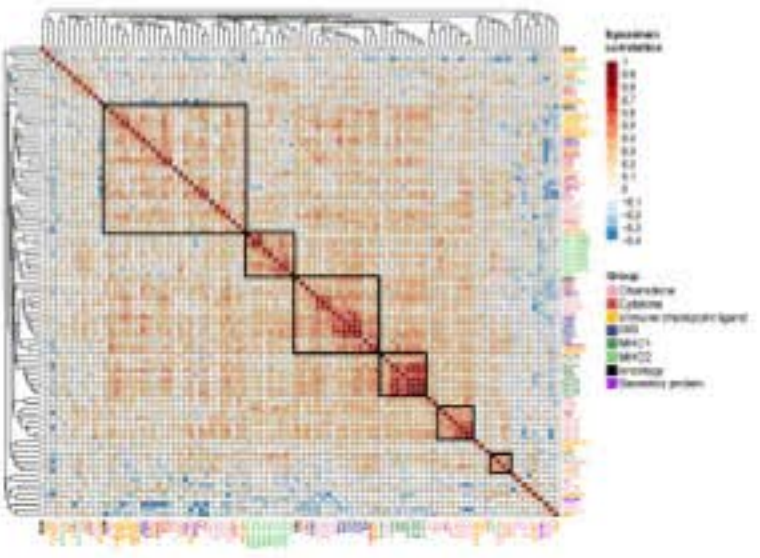

(b)

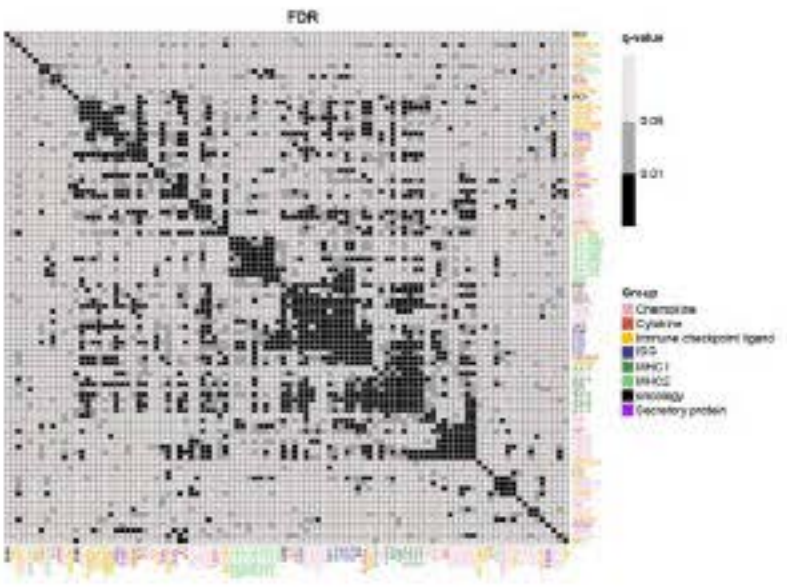

Figure 9. Identification of immune-modulatory regulons with genes in significant correlations. (a) Heatmap showing correlation between each immune-modulatory gene. Spearman correlation coefficient value was calculated to examine the co-regulatory relationships. Black box represents 6 different regulons including NK cell related regulon, MHC2 related regulon, LGALS9 related regulon, MHC1 related regulon, suppressive chemokine related regulon, and VTCN1 related regulon, starting from the left. **(b)** Heatmap illustrating FDR adjusted p-value for spearman correlation test between each immune-modulatory gene.

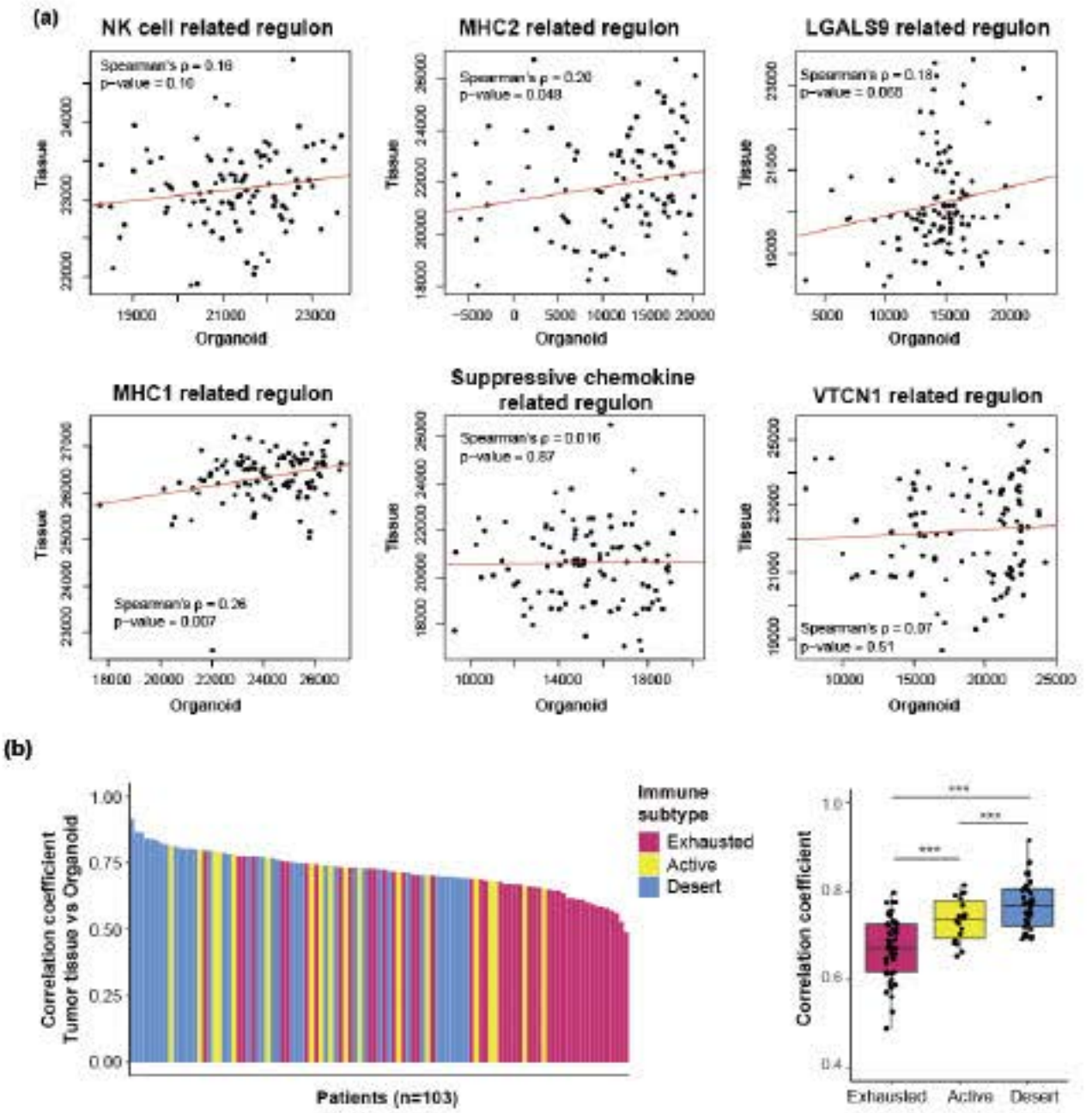

Figure 10. Correlation analysis of global regulon expression patterns in organoids and their corresponding tumor tissues. **(a)** A plot displaying ssGSEA score correlations for each regulon between organoids and tumor tissue, assessed using Spearman correlation analysis. **(b)** A plot showing Spearman correlation coefficient values for immune modulatory genes in 103 patients (left), with significance assessed using Wilcoxon rank-sum test (***$p < 0.001$) to compare differences between TIME groups (right). Data represents mean ± SD.

Table 1. A list of curated immune-modulatory genes

Group	Genes
MHCI (n = 8)	HLA-A, HLA-B, HLA-C, HLA-E, HLA-F, HLA-G, B2M, TAP2
MHC2 (n = 12)	HLA-DRA, HLA-DRB5, HLA-DRB1, HLA-DQB1, HLA-DOB, HLA-DMB, HLA-DMA, HLA-DOA, HLA-DPA1, HLA-DPB1, CIITA, CD74
Immune checkpoint ligand (n =19)	NECTIN4, PDCD1LG2, PVR, CD276, VTCN1, NECTIN3, NECTIN2, CEACAM1, CEACAM5, LGALS9, LGALS3, TNFRSF14, FGL1, CD86, CD274, CLEC2D, HHLA2, NCR3LG1, NID1
Interferon-stimulated gene (ISG) (n =8)	ISG15, ISG20, IFI6, IFI44, OASL, IFIT1, IFIT2, IFIT3
Chemokine (n = 30)	CCL2, CCL5, CCL14, CCL15, CCL20, CCL22, CCL24, CCL25, CCL26, CCL28, RARRES2, CX3CL1, CXCL1, CXCL2, PF4, CXCL5, CXCL6, PPBP, CXCL9, CXCL10, CXCL11, CXCL14, CXCL16, CXCL8, CSF2, MDK, MIF, CXCL17, CXCL3, CXCL12
Cytokine (n = 14)	IL10, IL16, BDNF, FSTL1, IL15, LIF, SPARC, IL1B, CHI3L1, IL18, CSF1, TNF, TNFSF10, IL1A
Secretory protein (n =4)	TGFB1, TGFA, VEGFA, GDF15
Oncology related protein (n = 3)	IDO1, MICA, MICB

Table 2. Lists of immune-regulatory genes included in 6 distinct regulons

NK cell related regulon	LGALS9 related regulon	MHC1 related regulon	MHC2 related regulon	Suppressive chemokine related regulon	VTCN1 related regulon
MICA	IDO1	HLA-G	HLA-DQB1	CCL2	CD74
CCL28	IL15	CSF2	HLA-DRB5	TNF	RARRES2
TNFRSF14	CSF1	HLA-A	HLA-DRB1	CCL20	CXCL6
LGALS3	ISG15	B2M	HLA-DMB	CXCL2	VTCN1
HHLA2	CXCL11	TAP2	HLA-DMA	CXCL8	
CEACAM5	CXCL9	HLA-E	HLA-DPB1	CXCL1	
CEACAM1	CXCL10	HLA-C	HLA-DRA	CXCL3	
ISG20	CCL5	HLA-B	HLA-DPA1		
GDF15	OASL	HLA-F	CIITA		
CD276	IFI44				
SPARC	IFIT1				
IL1B	IFIT2				
IL1A	IFIT3				
MDK	IFI6				
CD274	TNFSF10				
TGFA	LGALS9				
NECTIN2					
TGFB1					
LIF					
IL18					
CXCL17					
CX3CL1					
CCL22					
CXCL16					
CHI3L1					
CCL26					
NECTIN4					

6. Correlation between immune-modulatory regulon expression patterns in distinct types of CRC and their unique TIME

To elucidate the role of cancer intrinsic immune modulatory regulons in shaping TIME, association between the expression of each regulon in organoids and distinct tumor immune microenvironment (TIME) compositions of their corresponding tumor tissue was investigated. First, I examined whether the expression pattern of each regulon in organoids correlate with the abundance of immune cells in their matched tumor tissue. The ssGSEA scores calculated in the organoids were used to represent the cancer intrinsic expression level of each regulon. The discrepancies in regulon scores across three immune subtypes were examined, revealing the significant difference between immune active and exhausted group in MHC2 regulon score (Figure 11a). This finding indicated that MHC2 regulon expression within cancer cell has association with immunologically active tumor tissue. Considering that distinct CMS types of tumors harbors different TIME features, a comparative analysis of regulon scores across 103 organoids representing different CMS types of tumors was conducted to elucidate the contribution of cancer intrinsic regulon expression in TIME composition. Among the 6 immune-modulatory regulons, the MHC2-related regulon score was significantly higher in CMS1 type compared to CMS4 type tumors (Figure 11b). As the key distinction between the heavily immune infiltrated CMS1 type tumor and CMS4 type tumor lies in the immune-exhausted features of CMS4 tumors, this again demonstrates that the upregulation of the MHC2-related regulon in colorectal cancer cells is associated with the enhanced anti-tumor immunity. Collectively, these observations reveal the distinct expression patterns of regulon expression within cancer cells have correlation with the unique TIME of CRC.

Furthermore, the direct association between cancer intrinsic immune-modulatory regulon expression and the abundance of distinct immune cell populations was investigated. The Spearman correlation coefficient values between regulon scores obtained from the organoids and immune cell scores estimated from their matched tissues were calculated,

revealing noteworthy relationships. For instance, VTCN1 regulon expression exhibited a clear positive correlation with naïve B cells, while displaying an apparent negative correlation with memory B cells (Figure 12). Intriguingly, the expression of MHC2-related regulon in cancer cells showed no association with conventional CD4+ T cell activity but demonstrated a significant correlation with gamma delta T ($T_{\gamma\delta}$) cells, reported for their unique role in building an anti-tumorigenic TME by displaying MHC-independent cytotoxicity[22] (Figure 12). In addition, four of the immune-modulatory regulons (NK cell-related regulon, LGALS9-related regulon, MHC2-related regulon, suppressive chemokine-related regulon), which collectively encompassed more than half of the curated immune modulatory genes (n=58), all exhibited negative correlations with activated memory CD4+ T cells (Figure 12). This implies that the CD4+ T cell-unfavorable TME in CRC does not stem from a single factor but results from a complex interplay of various elements. Taken together, these observations reveal the dynamic interactions between individual regulons and distinct immune cell components, underscoring the importance of understanding the collective roles of cancer-derived immune modulatory proteins in CRC.

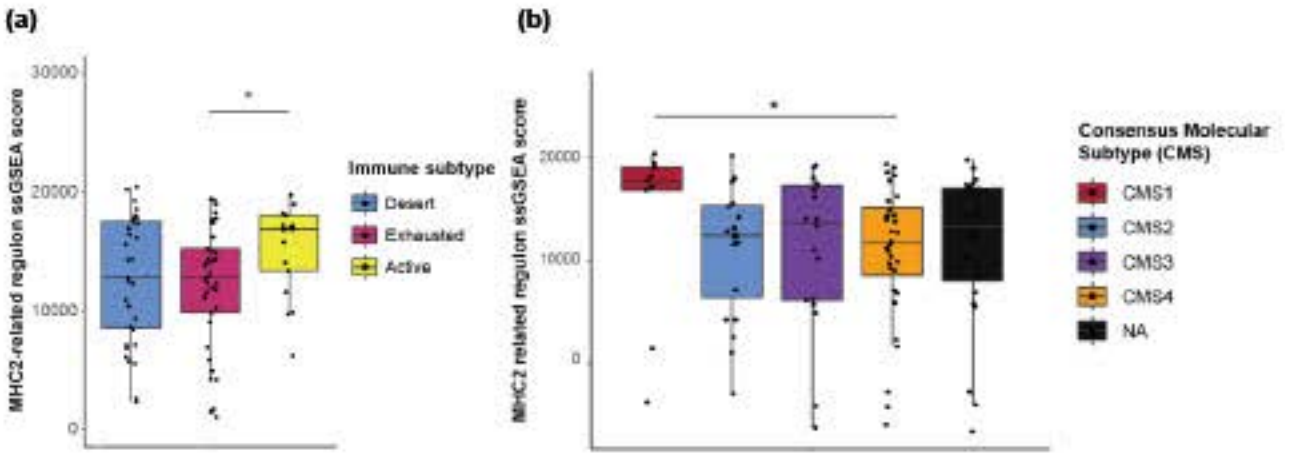

Figure 11. The expression of immune modulatory regulon in tumors of distinct immune status. (a) Plot showing the cancer-intrinsic expression level of the MHC2-related regulon, represented by the enrichment score calculated from the ssGSEA analysis with the transcriptomics data of 103 organoids across distinct immune subtypes (a) and distinct CMS types (b). CMS types were defined using bulk tumor tissue data. (a, b) Significance was assessed using Wilcoxon rank-sum test (*$p < 0.05$, **$p < 0.01$) to compare differences between the immune cold and immune hot groups (right). Data represents mean ± SD.

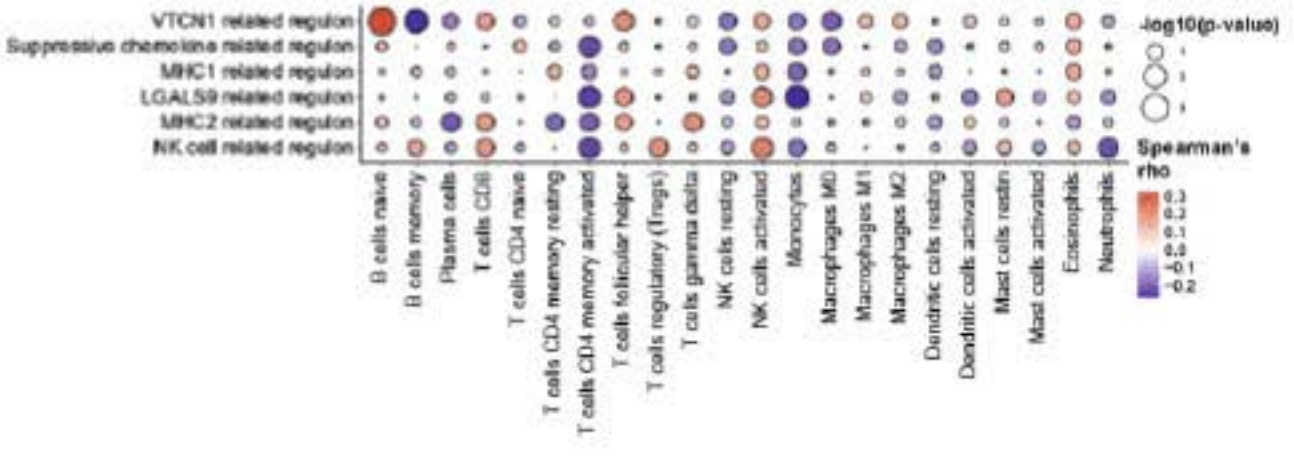

Figure 12. Correlation between regulon score in organoids and various immune cell populations. A bubble plot showing the correlation between the regulon ssGSEA scores computed for 103 organoids and the scores for 22 distinct immune cells calculated in 103 tumor tissues using CIBERSORT analysis.

7. Identification of candidate master regulators of immune-modulatory regulons

Focusing on the distinctive association of cancer-intrinsic MHC2 regulon expression with immune active group, CMS4 type tumors and $T_{\gamma\delta}$ cells, subsequent analysis was conducted to identify the candidate master regulator responsible for modulating the cancer intrinsic expression of this regulons. To do so, lists of transcription factors and their target gene pairs were collected from the Omnipath and Trrust (v2, human) database. In case of TFs collected from Trrust database, regulator, target protein pairs in both activation or suppression relationship were included. Target genes that share their upstream regulator were clustered as co-regulated regulon. Then, a hypergeometric test was conducted to determine the extent of overlap between genes identified within the MHC2-related regulon and the curated co-regulated regulons, revealing total 140 candidate master regulators (Table3).

Based on the assumption that the expression of master TFs of a given regulon would exhibit significant correlations with the expression patterns of genes comprising this regulon, I examined the correlation between the expression of 140 candidate master TFs and that of genes included in the MHC2-related regulon (Figure 13). Among various candidate TFs, a well reported TF of MHC2 encoding genes, *CIITA* showed overall significant and positive correlation with genes of MHC2-related regulon, supporting the validity of analysis (Figure 13). In addition to *CIITA*, *MITF* and *JUNB* expression in CRC organoids showed clear and positive correlation with MHC2-related regulon genes (Figure 13). Notably, the correlation analysis revealed SOX2 as the most likely candidate TF that suppresses the expression of cancer intrinsic MHC2-related regulon, indicated by the significant and negative correlation with multiple MHC2-related regulon comprising genes (Figure 13). Given the established notion in pro-tumorigenic function of SOX2 by inducing proliferation and drug resistance in cancer[23], the data from current study and accumulating reports rationalize further investigation on SOX2 as a potential targetable master regulator to enhance anti-tumor immune responses in CRC.

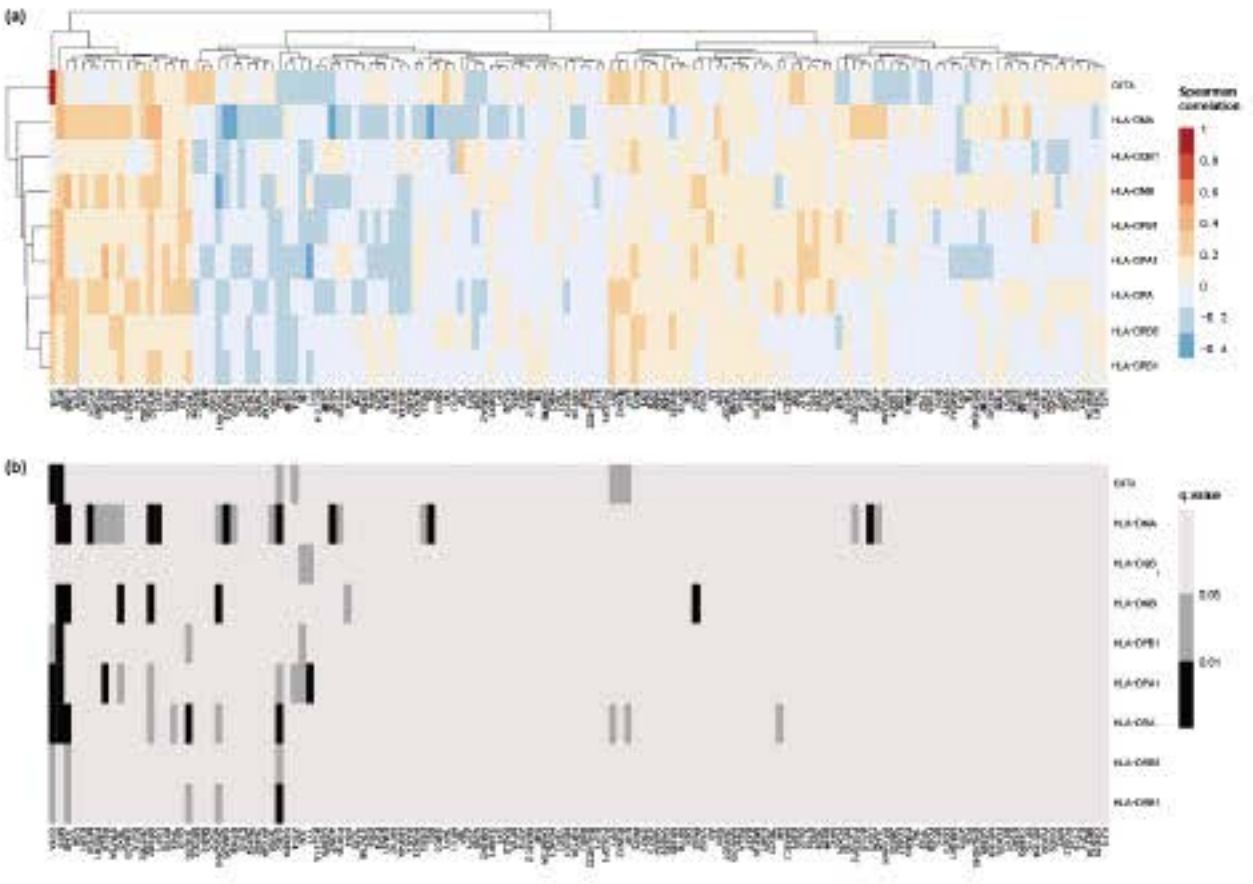

Figure 13. Correlation between genes in the MHC2-related regulon and their candidate regulators. (a) Heatmap showing the expression level correlation between immune-modulatory genes included in the MHC2-related regulon and their candidate regulators in the organoids. Spearman correlation analysis was conducted (b) Heatmap illustrating FDR adjusted p-value for spearman correlation test between each gene.

Table 3. Lists of candidate master regulators of MHC2-related regulon

TF	Overlapped genes	FDR
RFXANK	HLA-DQB1, HLA-DRB5, HLA-DRB1, HLA-DMB, HLA-DMA, HLA-DPB1, HLA-DRA, HLA-DPA1, CIITA	9.47E-32
RFXAP	HLA-DQB1, HLA-DRB5, HLA-DRB1, HLA-DMB, HLA-DMA, HLA-DPB1, HLA-DRA, HLA-DPA1, CIITA	9.47E-32
CHD2	HLA-DQB1, HLA-DRB1, HLA-DMB, HLA-DMA, HLA-DPB1, HLA-DRA, HLA-DPA1, CIITA	7.35E-29
RFX5	HLA-DQB1, HLA-DRB5, HLA-DRB1, HLA-DMB, HLA-DMA, HLA-DPB1, HLA-DRA, HLA-DPA1, CIITA	1.02E-28
SMC3	HLA-DQB1, HLA-DRB1, HLA-DMB, HLA-DMA, HLA-DPB1, HLA-DRA, HLA-DPA1, CIITA	6.73E-27
TAF1	HLA-DQB1, HLA-DRB1, HLA-DMB, HLA-DMA, HLA-DPB1, HLA-DRA, HLA-DPA1, CIITA	2.37E-26
BCL11A	HLA-DQB1, HLA-DRB1, HLA-DMB, HLA-DMA, HLA-DPB1, HLA-DRA, HLA-DPA1, CIITA	4.68E-26
EBF1	HLA-DQB1, HLA-DRB1, HLA-DMB, HLA-DMA, HLA-DPB1, HLA-DRA, HLA-DPA1, CIITA	2.39E-25
BATF	HLA-DQB1, HLA-DRB1, HLA-DMB, HLA-DMA, HLA-DPB1, HLA-DRA, HLA-DPA1, CIITA	2.61E-25
RAD21	HLA-DQB1, HLA-DRB1, HLA-DMB, HLA-DMA, HLA-DPB1, HLA-DRA, HLA-DPA1, CIITA	2.61E-25
ZEB1	HLA-DQB1, HLA-DRB1, HLA-DMB, HLA-DMA, HLA-DPB1, HLA-DRA, HLA-DPA1, CIITA	9.53E-25
POU2F2	HLA-DQB1, HLA-DRB1, HLA-DMB, HLA-DMA, HLA-DPB1, HLA-DRA, HLA-DPA1, CIITA	1.32E-24
MEF2A	HLA-DQB1, HLA-DRB1, HLA-DMB, HLA-DMA, HLA-DPB1, HLA-DRA, HLA-DPA1, CIITA	1.32E-24
PBX3	HLA-DQB1, HLA-DRB1, HLA-DMB, HLA-DMA, HLA-DPB1, HLA-DRA, HLA-DPA1	1.56E-24
TBP	HLA-DQB1, HLA-DRB1, HLA-DMB, HLA-DMA, HLA-DPB1, HLA-DRA, HLA-DPA1, CIITA	2.84E-24
PAX5	HLA-DQB1, HLA-DRB1, HLA-DMB, HLA-DMA, HLA-DPB1, HLA-DRA, HLA-DPA1, CIITA	1.25E-23
CIITA	HLA-DQB1, HLA-DRB5, HLA-DRB1, HLA-DMB, HLA-DMA, HLA-DPB1, HLA-DRA	2.52E-21
EP300	HLA-DQB1, HLA-DRB1, HLA-DMB, HLA-DMA, HLA-DPB1, HLA-DRA, HLA-DPA1, CIITA	6.37E-21
SRF	HLA-DQB1, HLA-DRB1, HLA-DMB, HLA-DMA, HLA-DPB1, HLA-DRA, HLA-DPA1	1.25E-20
YY1	HLA-DQB1, HLA-DRB1, HLA-DMB, HLA-DMA, HLA-DPB1, HLA-DRA, HLA-DPA1, CIITA	1.41E-20
SPI1	HLA-DQB1, HLA-DRB1, HLA-DMB, HLA-DMA, HLA-DPB1, HLA-DRA, HLA-DPA1, CIITA	1.91E-20
FOS	HLA-DQB1, HLA-DRB1, HLA-DMB, HLA-DMA, HLA-DPB1, HLA-DRA, HLA-DPA1, CIITA	1.90E-19
STAT3	HLA-DQB1, HLA-DRB1, HLA-DMB, HLA-DMA, HLA-DPB1, HLA-DRA, HLA-DPA1, CIITA	3.75E-19
CTCF	HLA-DQB1, HLA-DRB1, HLA-DMB, HLA-DMA, HLA-DPB1, HLA-DRA, HLA-DPA1, CIITA	3.77E-19
USF2	HLA-DQB1, HLA-DRB1, HLA-DMB, HLA-DMA, HLA-DPB1, HLA-DRA, HLA-DPA1	3.96E-19
NFKB1	HLA-DQB1, HLA-DRB1, HLA-DMB, HLA-DMA, HLA-DPB1, HLA-DRA, HLA-DPA1, CIITA	9.41E-17
SP1	HLA-DQB1, HLA-DRB1, HLA-DMB, HLA-DMA, HLA-DPB1, HLA-DRA, HLA-DPA1, CIITA	1.90E-15
STAT1	HLA-DRB1, HLA-DMB, HLA-DMA, HLA-DRA, HLA-DPA1, CIITA	7.75E-13
MAFK	HLA-DMB, HLA-DPB1, HLA-DPA1, CIITA	1.37E-12
RFX1	HLA-DMB, HLA-DPB1, HLA-DRA, CIITA	3.14E-12
TFAP2C	HLA-DMB, HLA-DPB1, HLA-DPA1, CIITA	6.55E-09
EGR1	HLA-DMA, HLA-DPB1, HLA-DPA1, CIITA	7.29E-08
FOSB	HLA-DQB1, HLA-DRB1, CIITA	8.15E-08
VSX2	HLA-DQB1, HLA-DRB1	9.07E-08
FOSL1	HLA-DQB1, HLA-DRB1, CIITA	1.74E-07
FOSL2	HLA-DQB1, HLA-DRB1, CIITA	2.31E-07
JUNB	HLA-DQB1, HLA-DRB1, CIITA	2.97E-07
THRA	HLA-DQB1, HLA-DRB1	4.87E-07
JUND	HLA-DQB1, HLA-DRB1, CIITA	7.71E-07
KMT2A	HLA-DRA, CIITA	7.71E-07
ILF3	HLA-DRB1, HLA-DRA	1.58E-06
CREB1	HLA-DQB1, HLA-DRA, CIITA	2.20E-06
CEBPA	HLA-DMB, HLA-DPB1, CIITA	4.41E-06
E2F1	HLA-DMA, HLA-DPB1, CIITA	8.23E-06
JUN	HLA-DQB1, HLA-DRB1, CIITA	1.02E-05
FOXP1	HLA-DMA, CIITA	2.01E-05
NANOG	HLA-DPB1, HLA-DPA1	2.48E-05
EZH2	HLA-DRA, CIITA	6.06E-05
MYCN	HLA-DRB1, CIITA	8.31E-05
TAL1	HLA-DRB1, CIITA	9.12E-05
FOXP3	HLA-DQB1, CIITA	0.000121302
VDR	HLA-DRB1, CIITA	0.000134387
NFKB2	HLA-DRB1, CIITA	0.000135776
GATA3	HLA-DQB1, CIITA	0.000291809
ZNF362	CIITA	0.000400726
HNF4A	HLA-DMA, CIITA	0.00047831
MYC	HLA-DRB1, HLA-DPB1	0.000505847
ESR1	HLA-DQB1, HLA-DMB	0.000556293
ETS1	HLA-DMA, CIITA	0.000624109
NR2C1	HLA-DRB1	0.00072257
NFX1	HLA-DRA	0.00072257
PHF20	CIITA	0.001049373
ZXDC	CIITA	0.001049373
ADNP	CIITA	0.001356018
ZNF92	CIITA	0.001356018
BHLHE22	CIITA	0.001596648
EHF	HLA-DRB1	0.001596648
SMAD5	CIITA	0.001596648
DEK	HLA-DQB1	0.001596648
GLI3	HLA-DRB1	0.001786395
NR1I3	HLA-DRB1	0.001786395
ZNF207	CIITA	0.001786395
TBX5	HLA-DQB1	0.001786395
HMGA2	HLA-DRA	0.001786395
RELA	HLA-DRB1, CIITA	0.002278684

ZKSCAN1	CIITA	0.002318855
PAX3	HLA-DQB1	0.002541644
ZNF24	CIITA	0.002541644
SSRP1	CIITA	0.002719264
ZBED1	CIITA	0.002719264
HR	CIITA	0.002719264
BHLHE40	CIITA	0.002884161
NR2C2	HLA-DRB1	0.002884161
NR1H3	HLA-DRB1	0.002884161
SPIB	CIITA	0.003072971
CEBPG	CIITA	0.003072971
DNMT3A	HLA-DRB1	0.003290557
RBPJ	CIITA	0.003753126
EPAS1	HLA-DRB1	0.003914097
NFYC	HLA-DRA	0.003914097
ELF1	CIITA	0.004112741
IRF8	CIITA	0.004683114
TBX21	CIITA	0.004683114
PRDM1	CIITA	0.004683114
MEF2C	CIITA	0.00481449
NFATC2	CIITA	0.00481449
TCF3	CIITA	0.004841663
STAT5B	CIITA	0.004841663
GLI2	HLA-DRA	0.004841663
NFATC1	CIITA	0.004841663
HMGA1	HLA-DRA	0.005177525
IRF4	CIITA	0.005177525
DDIT3	HLA-DRB1	0.00534052
RUNX2	CIITA	0.00539657
ESR2	HLA-DQB1	0.00539657
NR1H4	HLA-DRB1	0.00539657
IRF2	CIITA	0.005499966
ATF3	HLA-DRB1	0.005499966
TP63	HLA-DQB1	0.005599573
NFYB	CIITA	0.005599573
NR1I2	HLA-DRB1	0.006142387
STAT5A	CIITA	0.006422043
CEBPD	CIITA	0.006422043
BCL6	CIITA	0.006634176
NFYA	HLA-DRA	0.006634176
YBX1	HLA-DQB1	0.006634176
REST	CIITA	0.006651232
ATF1	CIITA	0.006651232
NFIC	CIITA	0.006651232
RARA	HLA-DRB1	0.006961265
RUNX3	CIITA	0.007266072
ATF4	HLA-DRB1	0.007860517
POU2F1	HLA-DRA	0.007860517
SMAD3	CIITA	0.007973776
ATF2	CIITA	0.008368599
SOX2	CIITA	0.008368599
KLF4	CIITA	0.008819773
RELB	HLA-DRB1	0.010971504
E2F4	HLA-DMA	0.012071251
IRF1	CIITA	0.012146255
HDAC1	HLA-DRA	0.012220092
REL	HLA-DRB1	0.012623258
MITF	HLA-DMA	0.013184046
USF1	CIITA	0.013248302
PPARG	CIITA	0.01363435
GATA2	HLA-DPA1	0.014334688
CEBPB	CIITA	0.014706636
FOXA1	HLA-DQB1	0.017906389
AR	CIITA	0.025244305
TP53	HLA-DRB1	0.033344591

IV. DISCUSSION

While immunotherapies, including immune checkpoint ligands, have garnered significant interest in cancer treatment in both clinical practice and academia, their application in colorectal cancer (CRC) remains challenging[24]. Extensive research has confirmed that the majority of CRC cases exhibit tumor tissue with limited immune infiltration within the tumor immune microenvironment (TIME), contributing to the pronounced resistance of CRC to immunotherapies[25]. Therefore, understanding the cancer intrinsic features that contribute to the formation of an immune-unfavorable TIME would lay the foundation for enhancing the therapeutic efficacies of immunotherapy in CRC. However, due to the heterogeneous immune cell profiles within the tumor microenvironment (TME) among CRC patients and the complex interplay of multiple factors in TIME formation[26], targeting a single component or gene may not be sufficient to induce an immune-favorable TME.

In this research, the co-regulatory relationships among multiple cancer-intrinsic immune-modulatory genes were studied by analyzing gene expression data from 103 colorectal cancer patient-derived organoids and their corresponding tumor tissues. After confirming the correspondence of gene expression patterns related to carcinogenesis between the organoids and their matched tumor tissues, CRC tumors were classified into three immune subtypes based on their bulk tumor transcriptomic profiles and the infiltration levels of immune-stromal components. Intriguingly, the examination of CRC organoids across immune subtypes revealed distinct cancer-associated signaling pathway activation patterns in each immune subtype. Furthermore, co-regulatory relationships between immune response-related genes within CRC cells were investigated, leading to the identification of six different co-varying sets of immune gene modules. After confirming the associations with distinct immune cells for these regulons, the investigation extended to discover the upstream master regulator, revealing candidate targets that could be further studied for their cancer-intrinsic role in eliciting anti-tumor immunity in CRC.

While the current focus on enhancing anti-tumor immunity in CRC predominantly

revolves around the activation of CD8+ T cells, recent studies have underscored the multifaceted roles of various immune cell types, including gamma delta T (Tγδ) cells[27], myeloid-derived suppressor cells (MDSCs)[28], NK cells[29], and tumor-associated macrophages (TAMs)[30] in cancer. Together with these findings, the observations in the current study revealed a consistent negative correlation between overall regulons and the subset of activated memory CD4+ T cells, suggesting a prevailing T cell-unfavorable tumor immune microenvironment (TIME) in CRC (Figure 12). Given the well-established role of CD4+ T cells in bridging innate and adaptive immune responses, these results propose a plausible hypothesis for comprehending the anti-inflammatory nature of CRC.

Notably, the counterintuitive role of both anti-tumorigenic and pro-tumorigenic immune cells may underlie comparable expressions of immune-modulatory regulons in immune-cold and immune-hot types of tumors. Although the association of each cancer intrinsic immune modulatory regulon with the specific types of immune cell components harboring a distinct role was assessed, limitations in the type of immune cell estimation necessitate further research into how the regulons are involved in the recruitment and differentiation of the distinct subclasses of both innate and adaptive immune cell components. Additionally, despite the discovery of SOX2 as a potential target in overcoming challenges in CRC treatment with immunotherapies by modulating the expression of MHC2-related regulon, further experimental validation is yet required. This entails confirming the molecular-level expression of the regulon in the organoids and validating the regulator-regulon relationship between SOX2 and genes comprising MHC2-related regulon within CRC cells. In addition to molecular-level validations, further investigations into the specific outcomes of interactions between the identified regulon and distinct immune cell populations, which collectively shape a unique TIME, may bridge the gap between current research and clinical applications in immunotherapy.

V. CONCLUSION

In this study, the analysis of gene expression in tumor tissues identified three immune subtypes—exhausted, active, and cold—each associated with unique tumor stages and immune responses. By incorporating transcriptomics data from colorectal cancer (CRC) patient-derived organoids (PDOs), I discovered distinct cancer-associated signaling pathway activation patterns across immune subtypes. Investigating co-regulatory relationships among immune-modulatory genes within CRC PDOs identified six immune modulatory regulons associated with distinct immune subtypes and components of tumor tissues. Finally, I proposed a potential targetable master regulator of the MHC2-related regulon, suggesting a promising avenue for the concurrent modulation of cancer-derived immune inhibitory proteins and the comprehension of the immune microenvironment in heterogeneous CRC.

REFERENCES

(1) Yarchoan M, Hopkins A, Jaffee EM. Tumor Mutational Burden and Response Rate to PD-1 Inhibition. N Engl J Med. 2017;377(25):2500-2501.

(2) Grasso CS, Giannakis M, Wells DK, Hamada T, Mu XJ, Quist M, et al. Genetic Mechanisms of Immune Evasion in Colorectal Cancer. Cancer Discov. 2018;8(6):730-749.

(3) Spranger S, Bao R, Gajewski TF. Melanoma-intrinsic β-catenin signalling prevents anti-tumour immunity. Nature. 2015;523(7559):231-5.

(4) Neupane P, Mimura K, Nakajima S, Okayama H, Ito M, Thar Min AK, et al. The Expression of Immune Checkpoint Receptors and Ligands in the Colorectal Cancer Tumor Microenvironment. Anticancer Res. 2021;41(10):4895-4905.

(5) Lu Z, Zhao ZX, Cheng P, Huang F, Guan X, Zhang MG, et al. B7-H3 immune checkpoint expression is a poor prognostic factor in colorectal carcinoma. Mod Pathol. 2020;33(11):2330-2340.

(6) Zhang Z, Su T, He L, Wang H, Ji G, Liu X, et al. Identification and functional analysis of ligands for natural killer cell activating receptors in colon carcinoma. Tohoku J Exp Med. 2012;226(1):59-68.

(7) Kim J, Koo BK, Knoblich JA. Human organoids: model systems for human biology and medicine. Nat Rev Mol Cell Biol. 2020;21(10):571-584.

(8) Aran D, Hu Z, Butte AJ. xCell: digitally portraying the tissue cellular heterogeneity landscape. Genome Biol. 2017;18(1):220.

(9) Bindea G, Mlecnik B, Tosolini M, Kirilovsky A, Waldner M, Obenauf AC, et al. Spatiotemporal dynamics of intratumoral immune cells reveal the immune landscape in human cancer. Immunity. 2013;39(4):782-95.

(10) Charoentong P, Finotello F, Angelova M, Mayer C, Efremova M, Rieder D, et al. Pan-cancer Immunogenomic Analyses Reveal Genotype-Immunophenotype Relationships and Predictors of Response to Checkpoint Blockade. Cell Rep.

2017;18(1):248-262.

(11) Rooney MS, Shukla SA, Wu CJ, Getz G, Hacohen N. Molecular and genetic properties of tumors associated with local immune cytolytic activity. Cell. 2015;160(1-2):48-61.

(12) Tirosh I, Izar B, Prakadan SM, Wadsworth MH 2nd, Treacy D, Trombetta JJ, et al. Dissecting the multicellular ecosystem of metastatic melanoma by single-cell RNA-seq. Science. 2016;352(6282):189-96.

(13) Nirmal AJ, Regan T, Shih BB, Hume DA, Sims AH, Freeman TC. Immune Cell Gene Signatures for Profiling the Microenvironment of Solid Tumors. Cancer Immunol Res. 2018;6(11):1388-1400.

(14) Jiang P, Gu S, Pan D, Fu J, Sahu A, Hu X, Li Z, Traugh N, Bu X, Li B, Liu J, Freeman GJ, Brown MA, Wucherpfennig KW, Liu XS. Signatures of T cell dysfunction and exclusion predict cancer immunotherapy response. Nat Med. 2018;24(10):1550-1558.

(15) Cho EJ, Kim M, Jo D, Kim J, Oh JH, Chung HC, et al. Immuno-genomic classification of colorectal cancer organoids reveals cancer cells with intrinsic immunogenic properties associated with patient survival. J Exp Clin Cancer Res. 2021;40(1):230

(16) Zhang Y, Zhang Z. The history and advances in cancer immunotherapy: understanding the characteristics of tumor-infiltrating immune cells and their therapeutic implications. Cell Mol Immunol. 2020;17(8):807-821.

(17) Mhaidly R, Mechta-Grigoriou F. Role of cancer-associated fibroblast subpopulations in immune infiltration, as a new means of treatment in cancer. Immunol Rev. 2021;302(1):259-272.

(18) Picard E, Verschoor CP, Ma GW, Pawelec G. Relationships Between Immune Landscapes, Genetic Subtypes and Responses to Immunotherapy in Colorectal Cancer. Front Immunol. 2020;11:369.

(19) van den Elsen PJ. Expression regulation of major histocompatibility complex class I and class II encoding genes. Front Immunol. 2011;2:48.

(20) Humblin E, Kamphorst AO. CXCR3-CXCL9: It's All in the Tumor. Immunity. 2019;50(6):1347-1349.

(21) Reschke R, Yu J, Flood B, Higgs EF, Hatogai K, Gajewski TF. Immune cell and tumor cell-derived CXCL10 is indicative of immunotherapy response in metastatic melanoma. J Immunother Cancer. 2021;9(9):e003521.

(22) Park JH, Lee HK. Function of γδ T cells in tumor immunology and their application to cancer therapy. Exp Mol Med. 2021;53(3):318-327.

(23) Zhang S, Xiong X, Sun Y. Functional characterization of SOX2 as an anticancer target. Signal Transduct Target Ther. 2020;5(1):135.

(24) Shan J, Han D, Shen C, Lei Q, Zhang Y. Mechanism and strategies of immunotherapy resistance in colorectal cancer. Front Immunol. 2022;13:1016646.

(25) Yuan J, Li J, Gao C, Jiang C, Xiang Z, Wu J. Immunotherapies catering to the unmet medical need of cold colorectal cancer. Front Immunol. 2022;13:1022190.

(26) Pelka K, Hofree M, Chen JH, Sarkizova S, Pirl JD, et al. Spatially organized multicellular immune hubs in human colorectal cancer. Cell. 2021;184(18):4734-4752.e20. doi: 10.1016/j.cell.2021.08.003.

(27) Sebestyen Z, Prinz I, Déchanet-Merville J, Silva-Santos B, Kuball J. Translating gammadelta (γδ) T cells and their receptors into cancer cell therapies. Nat Rev Drug Discov. 2020;19(3):169-184.

(28) Wu Y, Yi M, Niu M, Mei Q, Wu K. Myeloid-derived suppressor cells: an emerging target for anticancer immunotherapy. Mol Cancer. 2022;21(1):184.

(29) Myers JA, Miller JS. Exploring the NK cell platform for cancer immunotherapy. Nat Rev Clin Oncol. 2021;18(2):85-100.

(30) Kloosterman DJ, Akkari L. Macrophages at the interface of the co-evolving cancer ecosystem. Cell. 2023;186(8):1627-1651.

ABSTRACT(IN KOREAN)

대장암 오가노이드 기반 암세포 내재적 면역회피 레귤론 규명 및 면역저항 조절전략 도출 대장암 오가노이드 기반 암세포 내재적 면역회피 레귤론 규명 및 면역저항 조절전략 도출

<지도교수 김현석>

연세대학교 대학원 의과학과

김 민 지

대장암(Colorectal cancer, CRC)은 면역억제 특성을 가진 암 종류로 알려져 있으며, 5%만이 면역 치료제에 반응성을 띄는 것으로 알려져 있다. 이에 따라, 종양 면역 미세 환경(Tumor immune microenvironment, TIME)이 면역 치료제 반응성에 어떠한 영향을 미치는지에 대한 이해가 필요하지만, 종양 내재적 특성에 따른 상이한 면역 조절 단백질 발현과 이것이 유도하는 면역 세포 조성에 대한 이해는 아직 한정적이다. CRC에서의 면역 요법 내성 발달은 암세포의 고유한 특성에 따라 다른 메커니즘을 통해 발생한다는 바가 알려져 있다. 이는 암의 특성에 따른 다양한 면역 조절 메커니즘을 포괄적으로 이해하는 것이 중요함을 시사한다. 따라서, 본 연구는 대장암 내재적 특성과 더불어 환자 특이적 종양 이질성(heterogeneity)을 반영한 연구를 위해 환자 유래 오가노이드를 활용하고자 하였다. 100여명의 환자 유래 오가노이드 및 상응하는 종양조직의 전사유전체 분석을 통해 대장암 내제적 면역조절인자 및 분비단백질과 같은 다양한 면역조절단백질 집합체를 공동으로 조절하는 regulon을 발굴하고자 하였으며, 더 나아가 이러한 면역조절단백질들의 상위 전사인자를 규명함으로써 대장암에서 보다 효과적인 면역치료 접근법을 제시할 수 있을 것으로 기대한다.

핵심되는 말 : 종양 내제적, 면역 조절 레귤론, 대장암, 오가노이드